P. Aceti, C. Bianchi, G. Sala
Hygrothermal Effects in Aeronautical Composite Materials Subjected to Freeze–thaw Cycling
Aerotecnica, Missili e Spazio, 2023, p. 1-13
doi:10.1007/s42496-023-00190-5

Hygrothermal effects in aeronautical composite materials subjected to Freeze-Thaw cycling

Pietro Aceti[a,*], Christian Bianchi[a], Giuseppe Sala[a]

[a]*Department of Aerospace Science and Technology, Politecnico di Milano, Via La Masa,34, Milan, 20156, Italy.*
[*]*Corresponding author: pietro.aceti@polimi.it*

Abstract

Fiber-reinforced composites (FRC) have gained widespread recognition in the aerospace, automotive, and energy industries due to their exceptional strengthto-weight ratio. However, comprehending their performance within varying environmental contexts poses a multifaceted challenge. Specifically, the influence of humidity, temperature fluctuations, and freeze-thaw cycles on the structural integrity of FRC components requires careful examination. This research work seeks to provide insights into the effects of humidity, temperature, and freezethaw cycles on FRC inter-laminar regions and the critical matrix/fiber interface. The experimental methodology employed includes a comprehensive array of techniques, such as thermal analysis, X-Ray tomography, and ILSS mechanical testing. Through these methods, an effort is made to discern the material's response to the environmental variables. Carbon-reinforced composites exhibited a shear strength reduction of 16.9% at 80°C, and glass-reinforced composites displayed a reduction of 18.4%. Further increasing the temperature to 125°C resulted in a reduction of 32.5% for carbon-reinforced composites and 38.8% for glass-reinforced composites. In hot-wet conditions, which combine humidity saturation and a testing temperature of 80°C, the shear strength reductions were the most pronounced, with a reduction of 48.7% for carbon-reinforced composites and 60.2% for glass-reinforced composites. Moreover freeze-thaw cycle has been performed. The findings of this research endeavor hold profound implications for both the design and maintenance of FRC components. As FRCs continue to gain prominence in critical applications, an enhanced understanding of their behavior in diverse environmental conditions becomes increasingly imperative.

Keywords: Fibre reinforced composite, moisture absorption, freeze-thaw cycle

---

1. Introduction

Temperature and humidity can degrade the fiber/matrix interaction and deteriorate the matrix's physical properties. Studies have shown that the interlaminar regions and the matrix/fiber interface are vulnerable to moisture and temperature. Research explored the various processes by which moisture might impact composites' performance [1, 2, 3], The mechanical properties of the composite are more negatively influenced by the simultaneous presence of moisture and the freeze-thaw cycle than by any other environmental component alone. Microcracks are started by freeze-thaw cycles, which increases moisture penetration into composite structures [4]. The influence of temperature changes on the properties of FRP composites is the subject of intensive research and analysis for many years. Elevated temperature may result in a reduction of: fibre strength and stiffness, adhesion at the fibre/polymer matrix interface, and chemical and/or physical damage of the polymer matrix [5, 6, 7]. The causes of the mentioned forms of damage and degradation derive from weakening at the interface of the fiber and matrix, as well as high temperature-induced residual stresses in the polymer matrix.

Considering a commercial aircraft, it's fundamental to define the atmospheric conditions present at the flight level where is flying in order to predict the hygrothermal effects on the structure. The International Civil Aviation Organization (ICAO) established a standard temperature for aviation in order to set a baseline from which manufacturers could generate performance data that pilots all around the world could use. This standard temperature is known as the "ISA," or ICAO Standard Atmosphere.

The standard temperature in aviation is 15° C or 59° F and is measured at a pressure of 29.92 inches of mercury (Hg) at mean sea level (msl). The standard temperature drops by 2 degrees Celsius (3.5 degrees Fahrenheit) for every 1,000 feet climbed, and this is reasonably accurate up to 36,000 feet msl. The temperature zone between 36,000 and 80,000 feet msl is considered constant at roughly -55 °C or -65 °F [8].

The applied flight level during the cruising phase of the aircraft can be defined as "Requested Flight Level (RFL)". It is usually concentrated among a few major flight level zones which can be defined as "Major Requested Flight Level (MRFL) [9]. In the majority of cases the cruising flight level is between FL320 and FL400. For the ISA at this altitude the temperature encountered by a commercial civil aircraft are between -48°C and -55 °C. Considering the amount of flight that an aircraft has to perform during its life all the structural components are subjected to a huge number of freeze-thaw cycles.

Although the temperature of the static air at this altitude can be as low as -55°C the skin temperature of the aircraft in higher since a body moving through air and compressing it is going to cause the air temperature to rise. The maximum heat in an airplane occurs near the stagnation points. The kinetic energy of the flow is completely converted into pressure here, which heats the air and, as a result, the structure. Because of the low local speed and high pressure at and around the stagnation point, the rate of heat transfer is also high, adding to the heat load.

The formula for the stagnation point temperature T_s of an ideal gas of the temperature T_∞ hitting an object with the Mach number Ma is:

$$T_s = T_\infty - T_\infty \cdot \frac{(k-1) \cdot Ma^2}{2} \quad (1)$$

Commercial flights operate in transonic regime during cruise. The tip of the fuselage nose (stagnation point in the vehicle) of an airliner flying at Mach 0.85 will see the air temperature to rise. For air the ratio of specific heats k is 1.4. If we consider an aircraft flying at FL340 (34000ft) the static air temperature of the atmosphere is -55°C consequently the measured temperature at the tip would be equal to -23.48°C. This parameter is fundamental to dimension the freeze-thaw cycle.

The humidity absorption mechanism is described as a diffusion process. Diffusion is defined as the chemical process through which molecules of water tend to move spontaneously from an area of high concentration towards an area of low concentration, continuing until the gradient is leveled, when an equilibrium condition is reached. Diffusion mechanism is also recalled as an osmotic process, which is actually the spontaneous net movement or diffusion of solvent (water) molecules through a selectively permeable membrane from a region of high water potential to a region of low water potential, in the direction that tends to the equilibrium [10, 1]. The amount of moisture absorption in composites can be affected by several factors, including matrix and reinforcement properties, degree of cure, porosity, polarity, material homogeneity, environmental conditions (temperature, relative humidity), material condition, surface hygrophobicity after treatments, thickness, and design choices [11]. Because of the properties of the resin, composite materials are particularly vulnerable to moisture absorption. Indeed, the polymeric matrix employed in composite materials has a very hygrophilic behavior.

The hygrophilic nature typical of the polymers used for industrial composites depends on their morphology, which features significant porosities, voids and free spaces. Diffusion is promoted where there is enough porosity and voids within the material. For this reason, it is important to choose the appropriate type of resin [11]. Once a composite structure is exposed to a highly humid environment, due to the porosity and hygrophilic nature, water can diffuse inside until a saturation limit is reached. The absorbed moisture weight fraction can define how much water in respect to the total body weight of the structure is diffused through the porosity and voids of the material. As a result, the absorption rate is affected by the kind of polymer: if the molecules that compose the polymer chains are densely packed, empty spaces are minimized and diffusion is slowed.

Freeze-thaw cycles cause initiation of micro-cracks and therefore increase of moisture penetration into the composite structure increasing the absorbed moisture weight fraction after each phase change of absorbed water. Decrease of stiffness, strength, and strain energy release rate of composite by increasing the freeze-thaw cycles has been reported [4] [12].

2. Experimental program

2.1. ILSS test specimens and parameters

The ILSS specimens has been manufactured according to ASTM D2344/D2344M – 22. The geometry of the specimens are shown in Fig.1 [13].

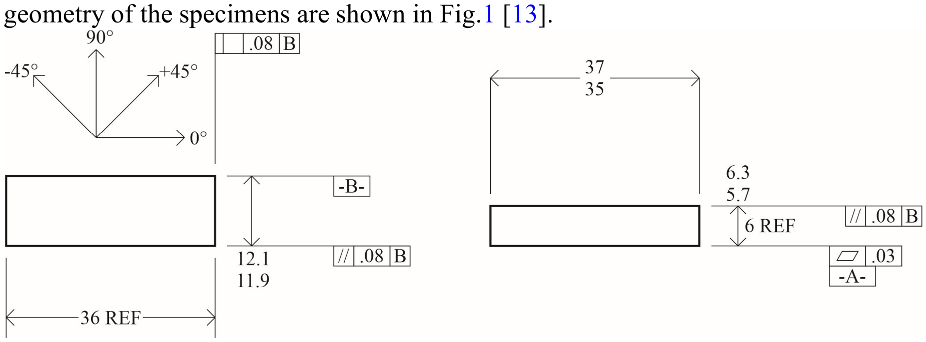

Figure 1: Standard geometry for specimen undergoing ILSS tests.

The thickness of the specimen is 6 mm, the width 12 mm and the length 36 mm. The specimens are cut from a composite panel made by overlapping 48 unidirectional plies at zero direction for carbon specimen and 24 for glass ones as shown in section 2.3. 72 carbon specimens and 72 glass specimens were manufactured and tested. A large variety of condition were tested.

2.2. Materials

Two typical aeronautical materials have been selected:

- **Carbon fibre prepeg**: composite prepreg carbon is a material used in the aeronautical field to manufacture lightweight, high-strength structures. It is made by impregnating carbon fibers with a thermoset resin. In our case plyes of unidirectional (UD) carbon prepegs are used with a thickness of 0.125mm;

- **Glass fiber prepeg**: Plyes of unidirectional (UD) glass prepegs are used with a thickness of 0.25mm.

2.3. *Fabrication of test specimens*

The following steps are followed in the manufacturing process of composite specimens:

1. Cutting: The prepreg material has been cut from a coil to get layers with a desired shape and orientation as shown in figure 2 a.
2. Lay-up: The prepreg material is arranged in a specified pattern and orientation as the initial step in the process to create the final product's desired shape. We will create two different panels with dimensions 190mm x 300mm;
3. Tooling: The prepreg lay-up is then placed on a tool, which is a mold or form that defines the shape of the final product. The mold used, shown in figure 2 b, was composed by a metal base and a metal counter mold. The final layup was placed inside a vacuum bag as shown in figure 2 c;
4. Autoclave: Once the lay-up is complete and placed on the tool, it is put into an autoclave, as shown in figure 2 d. The cycle is constantly monitored with the help of thermocouples placed inside the mold;
5. Curing: Usually, the curing process entails a series of temperature and pressure cycles, with the temperature and pressure gradually rising over time;
6. Trimming: The finished part is trimmed, from each panel we obtained more than 72 specimens. The cutting was performed with a circular saw equipped with a lubricated diamond blade as shown in figure 2 e. Each specimen was also trimmed to ASTM D2344/D2344M – 22 geometry, using a lapping machine.

The final results is shown in figure 2 f.

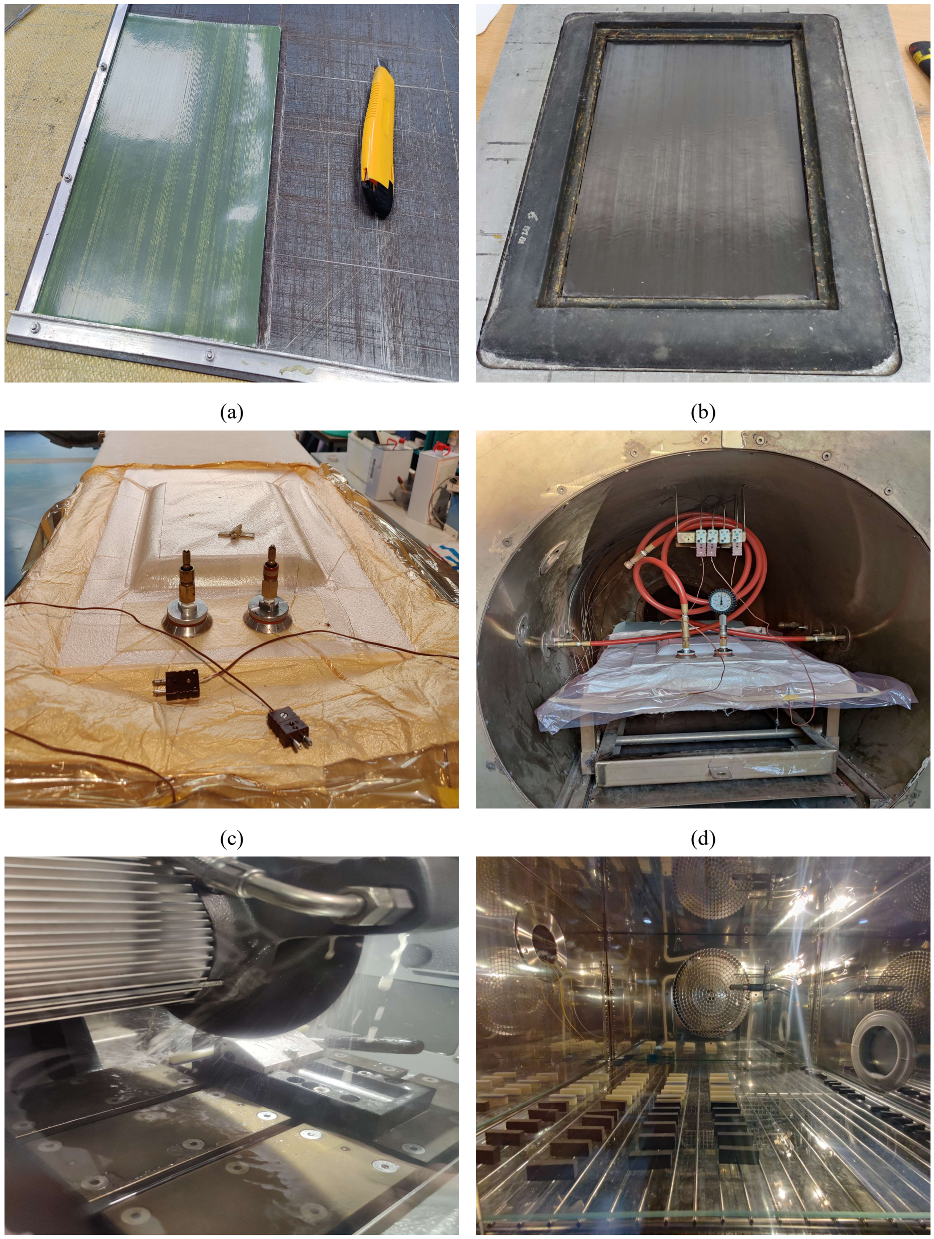

(a) (b) (c) (d) (e) (f)

Figure 2: Manufacturing process: prepregs cutting (a), Mold (b), vacuum bag (c), autoclave (d), circular saw (e), ILSS specimens (f)

2.3.1. Nomenclature of the specimen

In order to efficiently and correctly identify each specimen and which type of conditioning and testing occurred a nomenclature must be defined. The codes will be created similar to the following example: "EG-W-FT-50-D". The code is divided into five main blocks:

1. **Material discrimination**. In order to identify if we are working with fibre glass or carbon reinforced composite we identify "EG" as Epoxy Glass and "EC" as Epoxy Carbon;

2. **Conditioning**. A differentiation between specimen that are subjected to a conditioning process until saturation of the moisture and dry specimen must be done. To do so a “D” will represent a dry specimen that was subjected to the procedure D implemented in the standard procedure ASTM D5229/D5229M – 20 which goal is the reduction of humidity until a dry condition is obtained. A “W” will represent a wet specimen conditioned until saturation;
3. **Cycling and testing temperatures**. Two different thermal cycles will be performed. The first will guarantee a freeze condition of the water trapped inside the material as moisture and is characterized by a maximum temperature T = 30°C and a minimum temperature T = -22°C. In this case the nomenclature will state “FT” as Freeze-thaw cycle. The second cycle is characterized by two temperatures above the freezing condition, the nomenclature will state “HH” as Hot-hot cycle. The specimens will be subjected to a maximum temperature T = 30°C and a minimum temperature T = 5°C; the choice of these values is referred to the study of the typical flight of a general aviation aircraft [14]. Two different type of testing temperature will be performed on the material. In order to discriminate between the two different testing temperatures an “A”, for ambient and an “H” for hot will be added at the end. The ambient “A” will represent a laboratory temperature condition of T = 23°C with controlled humidity in range of 30% - 50%. The hot “H” temperature T = 70°C - 80°C. This temperature choice has to be made considering a considering an increase in temperature due to exposure of the aircraft structure to the sun in hot and humid areas of the earth (Singapore airport, case study);
4. **Number of cycles**. The number present at the end of the code will represent the number of cycles subjected to the material. In our experiment we performed a total of 10, 25, 50 and 100 cycles in order to better characterize the effect;

Code	No.	Material	Conditioning	Cycle Temps. (°C)	Test Temps. (°C)	No. of Cycles
EC-D-A	6	Epoxy-Carbon	No - Dry	NA	23	0
EC-D-H	6	Epoxy-Carbon	No - Dry	NA	70/80	0
EC-W-A	6	Epoxy-Carbon	No - Dry	NA	23	0
EC-W-H	6	Epoxy-Carbon	No - Dry	NA	70/80	0
EC-W-FTA-10	6	Epoxy-Carbon	Saturation	-22/30	23	10
EC-W-FTA-25	6	Epoxy-Carbon	Saturation	-22/30	23	25
EC-W-FTA-50	6	Epoxy-Carbon	Saturation	-22/30	23	50
EC-W-FTA-100	6	Epoxy-Carbon	Saturation	-22/30	23	100
EC-W-HHA-10	6	Epoxy-Carbon	Saturation	5/30	23	10
EC-W-HHA-25	6	Epoxy-Carbon	Saturation	5/30	23	25
EC-W-HHA-50	6	Epoxy-Carbon	Saturation	5/30	23	50
EC-W-HHA-100	6	Epoxy-Carbon	Saturation	5/30	23	100

Table 1: Fibre Carbon reinforced composites (FGRC) specimen nomenclature

Code	No.	Material	Conditioning	Cycle Temps. (°C)	Test Temps. (°C)	No. of Cycles
EG-D-A	6	Epoxy- Glass	No - Dry	NA	23	0
EG-D-H	6	Epoxy-Glass	No - Dry	NA	70/80	0
EG-W-A	6	Epoxy-Glass	No - Dry	NA	23	0
EG-W-H	6	Epoxy-Glass	No - Dry	NA	70/80	0
EG-W-FTA-10	6	Epoxy-Glass	Saturation	-22/30	23	10
EG-W-FTA-25	6	Epoxy-Glass	Saturation	-22/30	23	25
EG-W-FTA-50	6	Epoxy-Glass	Saturation	-22/30	23	50
EG-W-FTA-100	6	Epoxy-Glass	Saturation	-22/30	23	100
EG-W-HHA-10	6	Epoxy-Glass	Saturation	5/30	23	10
EG-W-HHA-25	6	Epoxy-Glass	Saturation	5/30	23	25
EG-W-HHA-50	6	Epoxy-Glass	Saturation	5/30	23	50
EG-W-HHA-100	6	Epoxy-Glass	Saturation	5/30	23	100

Table 2: Fibre Glass reinforced composites (FGRG) specimen nomenclature

3. Conditioning process

The most important environmental parameters influencing the degree of composite material degradation are relative humidity and temperature. Moisture impacts the resin in the first stage of the process, and then the interface region with the fibers in longer exposures to humid conditions. Temperature impacts the state of the moisture inside the composite, expanding during freezing condition and contracting during room temperature.

To define the initial reference condition of the specimen the procedure “D” of the Standard Test Method, D5229/D5229M - 20 [15], is used. This procedure covers the conditioning (drying) of material coupons to an essentially moisture-free condition. On each specimen this procedure is performed before the beginning of the moisture uptake process in order to be sure that the initial value of moisture uptake is zero.

3.1. Moisture uptake

Diffusion mechanism is recalled as an osmotic process, which is actually the spontaneous net movement or diffusion of solvent (water) molecules through a selectively permeable membrane from a region of high water potential to a region of low water potential, in the direction that tends to the equilibrium [10].

To perform the moisture uptake conditioning is followed the procedure “B” of the Standard Test Method, D5229/D5229M - 20 [15]. A conditioning chamber, shown in figure 3 a, with distilled water maintained at the temperature of 80°C, is used. The specimens are completely immersed in the water and weighted after defined intervals of time until saturation is reached. In order to do this, a stainless-steel specimen holder was fabricated and it’s shown in figure 3 b.

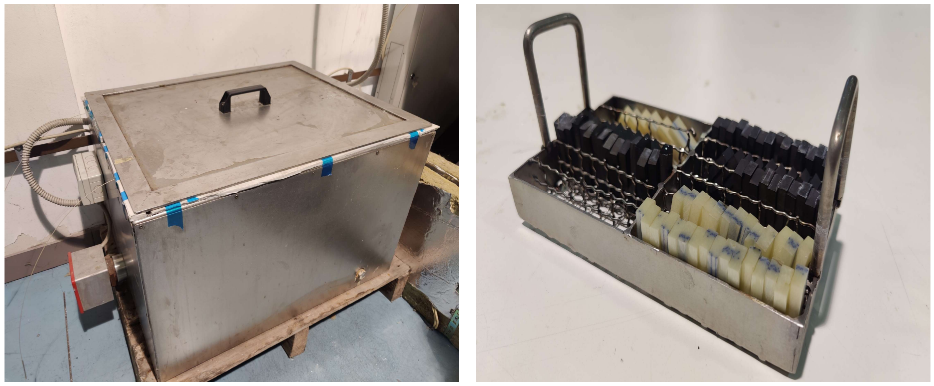

(a) (b)

Figure 3: Conditioning chamber (a) and specimens holder (b)

Figure 4 represents the moisture uptake of 60 FGRC specimen, which value was mediated among them.

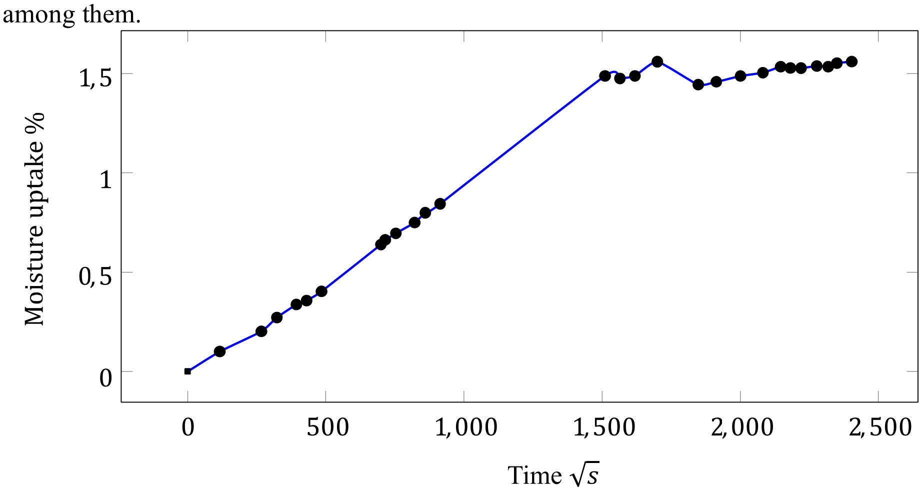

Figure 4: Moisture uptake of Fibre Glass reinforced composites (FGRC) specimens

Figure 5 and Figure 6 depict the moisture uptake behavior of FCRC specimens, with each graph corresponding to a different manufacturing method, but with the same material. Specifically, the first graph corresponds to specimens with fibers oriented along the 0° reference system (Figure 1), while the second graph corresponds to specimens, specially manufactured, with fibers oriented to the 90° direction (Figure 1).

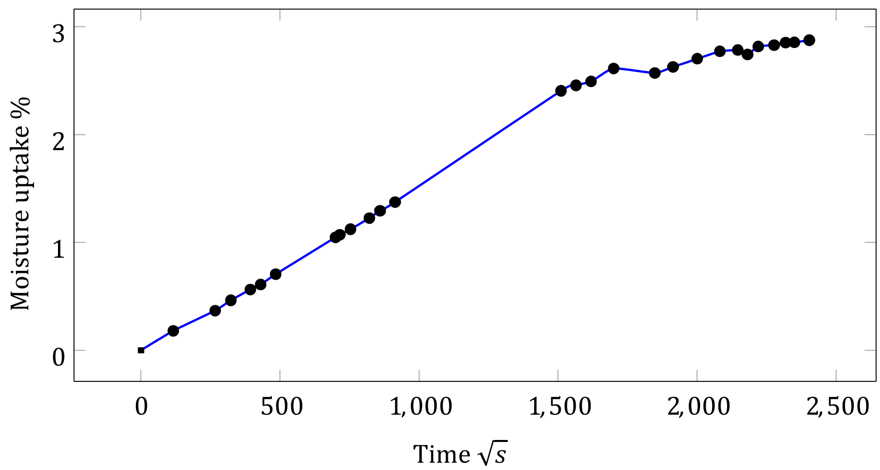

Figure 5: Moisture uptake of Fibre Carbon reinforced composites (FCRC) specimen-0°

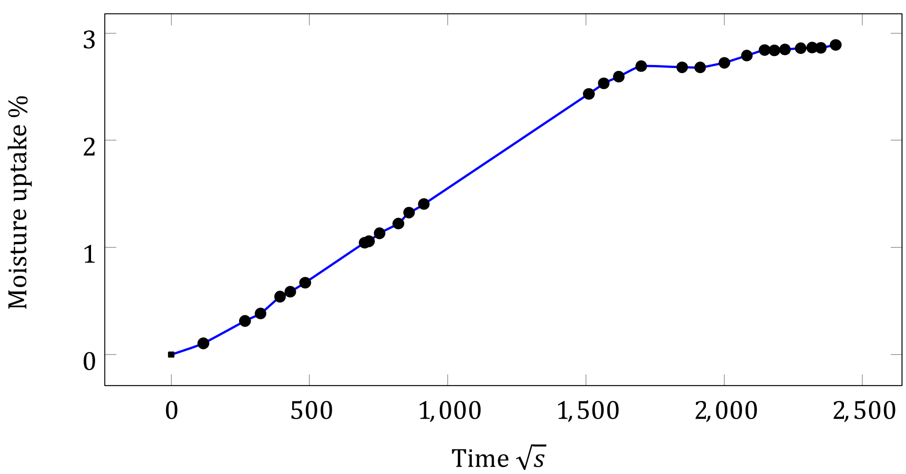

Figure 6: Moisture uptake of Fibre Carbon reinforced composites (FCRC) specimen-90°

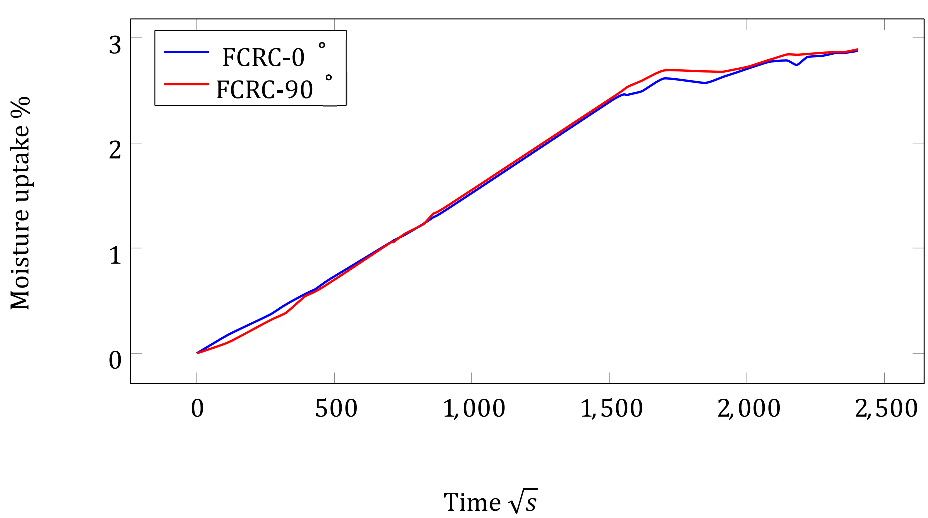

Figure 7: Moisture uptake confrontation FCRC-0° vs. FCRC-90°

In Figure 7 a confrontation between the two different specimen is presented. The data displayed indicate that both materials reached saturation after roughly thirty days. Also, we can see that for FCRC-0° and FCRC-90°, the orientation of the fiber in the plyes has little to no impact on the rate and nature of moisture absorption. This indicates that capillary absorption phenomena in sections with normal parallel to the fiber direction are negligible."

3.2. Thermal cycles

Commercial flights operate in transonic regime during cruise. The tip of the fuselage nose (stagnation point in the vehicle) of an airliner flying at Mach 0.85 will see air temperature to rise. For air the ratio of specific heats k is 1.4. If we consider an aircraft flying at FL340 (34000ft) the static air temperature of the atmosphere is -55°C consequently the measured temperature at the tip would be equal to -23.48°C.

In order to better characterize the testing conditions to subject the specimen in a series freeze-thaw cycles, a case study of the Singapore Changi Airport is conducted. In this particular location situated near the equator and has a typically tropical climate, with abundant rainfall, high and uniform temperatures, and high humidity all year round. Many of its climate variables, such as temperature and relative humidity, do not show large month-to-month variation. An average temperature of 30°C throughout the entire year is present and the mean annual relative humidity is 83.9%. Basing the choice of the maximum and minimum temperature on the data collected. According to the data gathered, a maximum cycle temperature of 30°C with an 83% percent humidity level and a minimum temperature of -22°C can be established [16],[17].

The temperature cycle is displayed in Figure 8 and is performed considering the ASTM Standard Practice for Freeze/Thaw Conditioning of Pultruded Fiber Reinforced Polymer (FRP) Composites Used in Structural Designs [18].

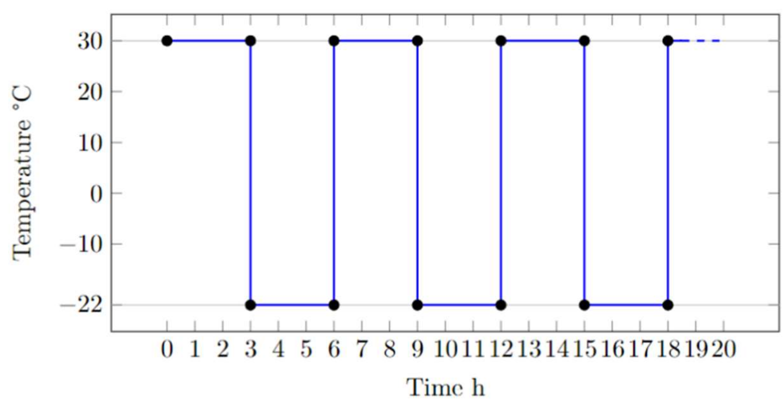

Figure 8: Freeze-Thaw cycles according to ASTM D7792/D7792M-15 [18]

The second temperature cycle is displayed in Figure 9 and is performed considering the case flight of a General aviation planes that typically cruise between 4500 and 9500 feet in altitude (data collected considering the datasheet of a Cessna-172 [14]).

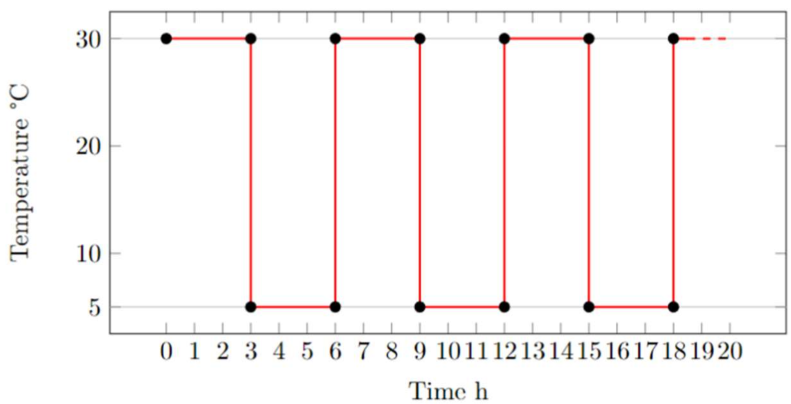

Figure 9: Thermal cycle without freezing condition of the specimen "Hot-Hot cycle".

4. Testing

4.1. Computed Tomography

X-ray computed tomography (CT) is becoming increasingly important among the non-destructive inspection techniques for applications where the three-dimensional (3D) nature of the phenomena is important, or where the evolution of critical features is of interest, either during manufacturing or under in-service conditions
[19].

In our experiments a North Star Imaging® X25 CT X-Ray Inspection, figure 10, system is used to inspect intralaminar damage due to conditioning and thermal cycling. All the 144 are tested before performing the mechanical ILSS test.

Figure 10: Tomography results on an FCRC (a) and FGRC (b) specimen tested in "wet" condition

The operation is accomplished in an automated way, being the X—rays emitting tube mounted on a robotized arm, supervised by a personal computer, which controls the tube rotations. Once performed, radiograms from two different angles are digitized, defects to be measured and located are interactively identified, and their through-the-thickness position is determined by trigonometric algorithms in a computer code that compares apparently different locations of the same defect in different radiograms [20]. The techniques works well also if material to be analyzed is notradio-opaque (as for example carbon fibers): in this case it previously moistened with a zinc—iodide solution, which penetrates defects by capillarity, making them visible to X-rays.

For non—radio—opaque thermosetting composite materials an opaque enhanced dye penetrant has been used [20], consisting of:

- 10ml of isopropyl alcohol;
- 10ml of distilled water;
- 1ml of Kodak® Photo Flo 200 wetting agent;
- 60mg of zinc iodide.

4.2. Mechanical tests (ILSS)

A shear test of a composite material is performed to determine the shear modulus or shear strength, or both. The in-plane shear modulus is denoted by G12, and the shear strength by S6. The major deficiency of all existing shear test methods for composite materials is the lack of a pure and uniform state of shear stress in the test section [21].

ILSS, ASTM D2344, short-beam shear test is an interlaminar shear test method. The specimen is constituted of (0°)n plies, where n is the number of plies that must be sufficient to induce enough shear load into the specimen. Nevertheless, the ASTM standard advocates the following beam theory formula for the maximum shear stress: [13]

$$\tau_{13} = \frac{3}{4} \cdot \frac{P}{A} \tag{2}$$

Where P is the applied load on the beam, and A is the cross-sectional area of the beam.

4.2.1. Test setup and instrumentation

The ASTM D2344/D2344M ”Short-Beam test” is conducted through usage of a MTS® 810 Material Test System Machine ref.318.25 (Figure 11), an uniaxial servo-hydraulic machine capable of extensive testing capabilities while featuring a load capacity up to 50 kN. The specimens are stored in a conditioned environment until test time and for each experiment an appropriate thermocouple is placed at specimen mid-length to monitor the temperature. The same thermocouple will be utilized to monitor the correct temperature during the “high-temperature” test, in which both the environment and specimen are heated and maintained at 80°C. Figure 12 depicts the infrared lights and their supports used to reach the previous environmental condition. The test speed is set at a rate of crosshead movement of 1.0 mm (0.05 in.)/min [13].

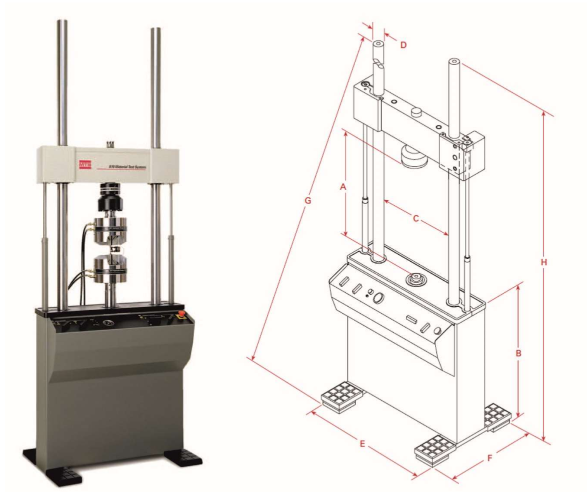

Model	318.25	
Force capacity (maximum)	250 kN	(55 kip)
Available actuator ratings	100, 250 kN (22, 55 kip)	
Vertical test space* (A)	1625 mm	(64 in)
Working height (B)	889 mm	(35 in)
Column spacing (C)	635 mm	(25 in)
Column diameter (D)	76 mm	(3 in)
Base width (E)	1003 mm	(39.5 in)
Base depth (F)	762 mm	(30 in)
Diagonal Clearance (G)	3251 mm	(128 in)
Overall Height (H)	3023 mm	(119 in)
Stiffness†	4.3×10^8 N/m	(2.4×10^6 lb/in)
Weight	910 kg	(2000 lb)

Figure 11: MTS® 810 Material Test System Machine.Adapted from [22]

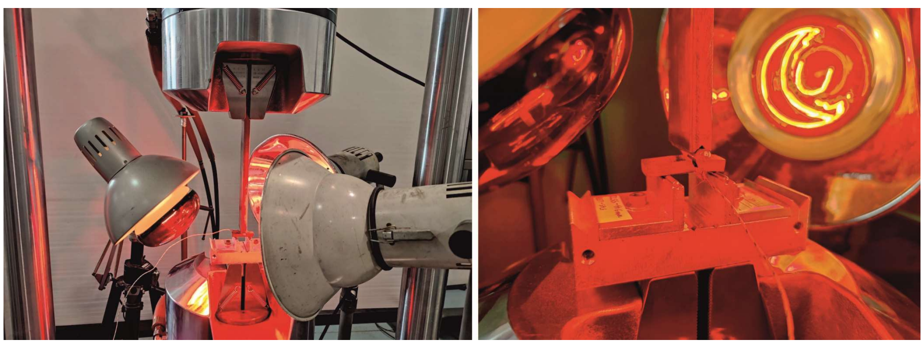

Figure 12: MTS® 810 Material Test System Machine with infrared lamps positioned to reach the goal testing temperature.

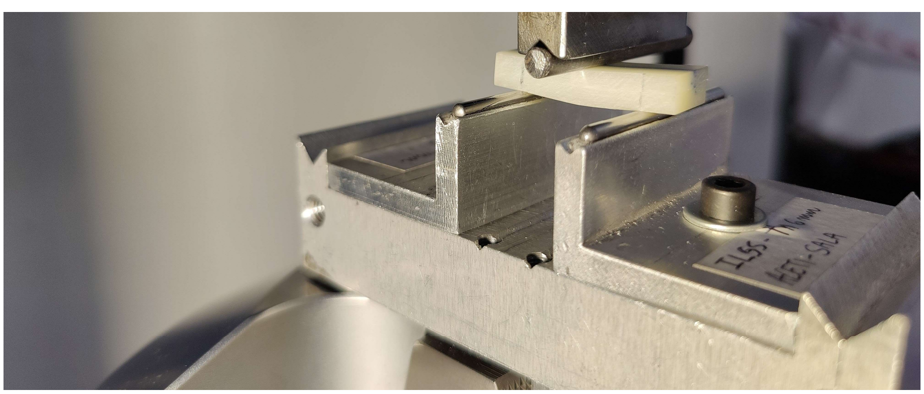

Figure 13: Short-Beam test performed on a FGRC specimen.

5. Results

5.1. Thermal Effects

Temperature has a significant impact on the mechanical properties of composite materials. The variations in temperature lead to transformations in the material's microstructure and properties, such as thermal expansion, deterioration, and softening [23]. To ensure precise testing, a reference condition is established for dry specimens at a standard temperature of 23°C, which serves as a baseline for future experiments. Carbon-reinforced and glass-reinforced composites are investigated, and their shear strengths are found to be $91.77 \pm 0.37 MPa$ and $72.52 \pm 1.72 MPa$, respectively, displaying a linear elastic phase followed by a sudden decrease in applied load until the fracture point, which is identified as correct in ASTM D2344/D2344M. The temperature-dependent behavior of composite materials is evaluated by performing tests at 23°C, 60°C, 80°C, 110°C, and 125°C. To rigorously assess the material's mechanical characteristics, additional test specimens were meticulously manufactured and then introduced into the originally anticipated set of 144 specimens. Each sample is heated in a convection oven, and infrared lights are employed during testing to maintain the desired temperature. The experimental imprecision is considered with the confidence interval, and interpolation curves are used to produce summary graphs depicting the mean shear stress, figure 14. Macroscopic investigation and XRay Tomography confirm the correct fracture behavior of the composites under various temperatures.

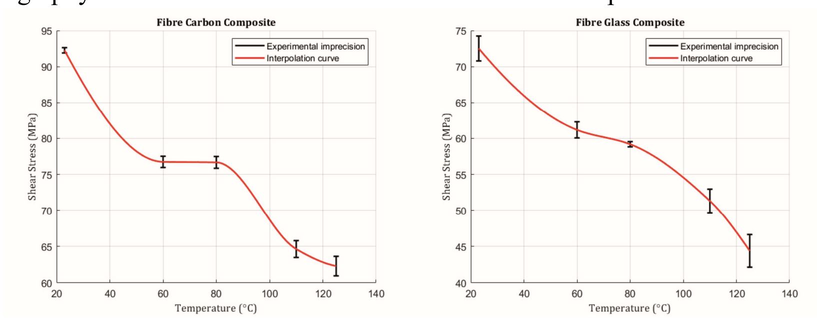

Figure 14: Interpolation ILSS results for FCRC and FGRC specimen tested at different temperatures.

5.2. Hygrothermal Effects

Plasticization occurs when water molecules are absorbed into a material, transitioning it from a glassy to a rubbery state. This results in enhanced chain mobility and weaken intermolecular bonds. Consequently, there is a decrease in strength modulus and stiffness, while toughness and strain capacity increase [1]. The ILSS test demonstrates that the carbon-reinforced composite exhibits plastic behavior with a less pronounced fracture compared to the dry material. Fracture occurs due to shear stress at the neutral mid-plane, confirmed by macroscopic examination, tomographic analysis figure 15 a, and slow-motion videos. In contrast, the glass fiber reinforced composite initially shows an elasto-brittle behavior and the expected failure mode according to ASTM D2344. However, further investigation reveals an incorrect failure mode during the ILSS test. The wet glass-reinforced specimen collapses at the center until buckling occurs, as observed through tomography figure 15 b.

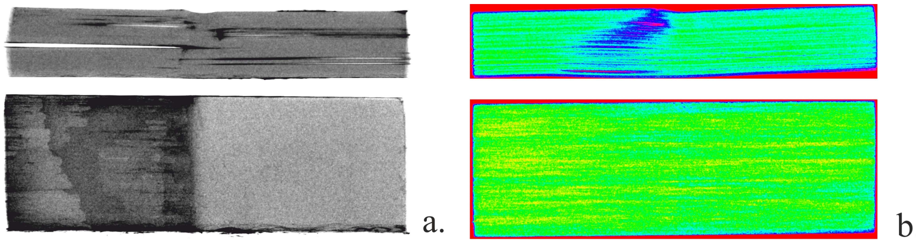

Figure 15: Tomography results on an FCRC (a) and FGRC (b) specimen tested in ”wet” condition

It is possible to identify the variation of the shear strength in relation to the different kinds of tests conditions in figure 16.

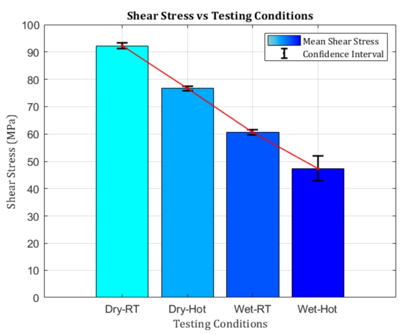

(a)

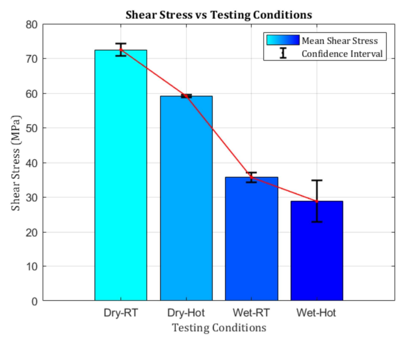

(b)

Figure 16: ILSS results for FCRC and FGRC in different test enviromental conditions.

5.3. Thermal cycling effect

A drying cycle is included in both types of cycles to restore the material to a dry condition once the cycle is completed. By removing the internal water in the composite, the impacts of the cycles can be isolated from the plasticization effects of the matrix. In figure 17 a and figure 17 b, it is possible to compare the “Freeze-Thaw” and ”Hot-Hot” cycling outcomes. According to our previous hypothesis, the results should demonstrate a clear distinction between the two curves indicating the severity of degradation caused by the “F-T” because of the nature of water expansion within the material. In contrast, the obtained results cannot demonstrate this phenomenon.

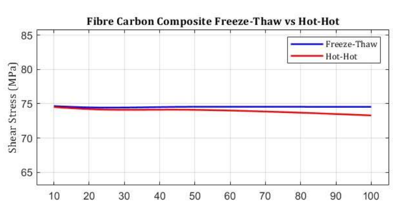

(a)

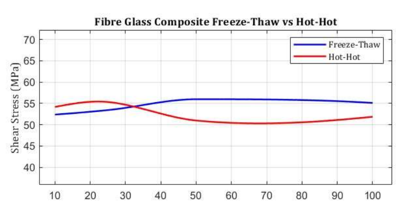

(b)

Figure 17: ILSS comparison for FCRC (a) and FGRC (b) ”F-T” vs ”H-H” cycling.

6. Conclusion

The study aimed to establish a representative coefficient that would indicate the extent to which the mechanical characteristics of the material deteriorate under harsh environmental conditions, in order to save time in the aeronautical industry when conducting destructive tests and to consider standard parameters for material strength loss in project planning. The research involved selecting two materials that are commonly utilized by aeronautical manufacturers: a carbon reinforced composite and a glass-reinforced composite. The Short Beam Shear Test "ILSS" was selected to investigate the phenomenon.

Findings revealed significant shear strength reduction in both materials compared to the dry condition. In fact, dry carbon specimens show a shear strength reduction of 16.9 % at 80°C, instead glass specimens show a reduction of 18.4%. By increasing the temperature up to 125°C, a value still below the glass transition temperature of the resin system, the reduction of shear strength is 32.5 % for carbon specimens and 38.8 % for glass ones. The "Hot-Wet" condition (combination of humidity saturation and testing temperature of 80°C) showing the most pronounced reduction of 48.7% for carbon specimens and 60.2% for glass ones. The results are shown in a graphical way in figure 16.

These results indicate that when designing an aeronautical component, in which the matrix-based characteristics are crucial, a correction factor of no less than 0.5 must be implemented. In such instances, the reinforcing fibers, whose objective in composite materials is to withstand axial loads, might be susceptible to buckling and instability as a consequence of the weakening of the epoxy resin's support.

Regarding the impact of thermal cycles on epoxy resin, it was not feasible to draw definitive and incisive conclusions concerning material deterioration due to humidity expansion. The existing literature indicates a reduction in shear strength of approximately -25% [4]. It is noteworthy that these findings were obtained using an epoxy resin designed for civil engineering structures, cured through out-of-autoclave techniques and with significantly lower structural shear properties compared to pre-peg aeronautical materials. Freeze-thaw cycles had a more significant impact on the matrix phase of the material in such cases, leading to substantial and visible deterioration of mechanical properties. The study focused on a maximum of 100 cycles, which represents a short interval in the operational lifespan of a commercial aircraft as per the case study on which this thesis is based. A total of 100 cycles in a medium-haul aircraft correspond to a month's worth of flights, and with an anticipated lifespan of nearly 30 years, the study investigated the beginning of the vehicle's life. Therefore, it is necessary to conduct research on the impact of a large number of cycles. It is important to investigate the possibility of reducing the duration of the temperature plateau in order to accelerate the cycling process, which may help to expedite the testing of a large number of cycles.

In light of the future prospects for further development of previous research, it would be of great interest to explore the absorption coefficient of humidity in composite materials coated with aeronautical paint. This aspect is a natural extension of the case study that was conducted with reference to commercial aviation. The objective of such a study would be to evaluate the effectiveness of paint and protective coatings on aircraft structures that are predominantly composed of composite materials. Furthermore, conducting investigations concerning the consequences of a saline environment in close proximity to seashore airports or aircraft carrier decks would be highly intriguing. The deteriorative potential of salt on metallic structures is a well-established fact, and it is crucial to conduct further and extensive research on composite materials and the efficacy of protective paint coatings.

7. Conflict of interest statement

On behalf of all authors, the corresponding author states that there is no conflict of interest.

8. OrcID

Pietro Aceti 0000-0003-3197-6009
Chrisitan Bianchi 0009-0002-6813-805X
Giuseppe Sala 0000-0003-1997-6073

References

[1] Pietro Aceti, Luca Carminati, Paolo Bettini, and Giuseppe Sala. Hygrothermal ageing of composite structures. part 1: Technical review. *Composite Structures*, 319:117076, 2023.

[2] I Barcelos Carneiro M Rocha, S Raijmaekers, RPL Nijssen, FP Van der Meer, and Lambertus J Sluys. Hygrothermal ageing behaviour of a glass/epoxy composite used in wind turbine blades. *Composite Structures*, 174:110–122, 2017.

[3] Chi-Hung Shen and George S Springer. Moisture absorption and desorption of composite materials. *Journal of composite materials*, 10(1):2–20, 1976.

[4] Mohammad Abedi, S. Ebrahim Moussavi Torshizi, and Roohollah Sarfaraz. Damage mechanisms in glass/epoxy composites subjected to simultaneous humidity and freeze-thaw cycles. *Engineering Failure Analysis*, 120:105041, 2 2021.

[5] Katarzyna Majewska, Magdalena Mieloszyk, Michal Jurek, and Wieslaw Ostachowicz. Coexisting sub-zero temperature and relative humidity influences on sensors and composite material. *Composite Structures*, 260:113263, 3 2021.

[6] WL Bradley and TS Grant. The effect of the moisture absorption on the interfacial strength of polymeric matrix composites. *Journal of materials science*, 30:5537–5542, 1995.

[7] ERK Chandrathilaka, JCPH Gamage, and Sabrina Fawzia. Mechanical characterization of cfrp/steel bond cured and tested at elevated temperature. *Composite Structures*, 207:471–477, 2019.

[8] Storm Dunlop. *A Dictionary of Weather*. Oxford University Press, ed.2 edition, 1 2008.

[9] ICAO. Analysis on flight level usage of major routes in sanya fir . in discussion on pbn routes development and flas/flos optimization. International Civil Aviation Organization, 2018.

[10] Afshin Bayatpour. Moisture effects on properties of polymeric composite laminates with different void content., 2019.

[11] Pietro Aceti, Luca Carminati, Paolo Bettini, and Giuseppe Sala. Hygrothermal ageing of composite structures. part 2: Mitigation techniques, detection and removal. *Composite Structures*, 319:117105, 2023.

[12] Laurent Cormier and Simon Joncas. Effects of cold temperature, moisture and freeze-thaw cycles on the mechanical properties of unidirectional glass fiber-epoxy composites. American Institute of Aeronautics and Astronautics, 4 2010.

[13] ASTM International. Standard test method for short-beam strength of polymer matrix composite materials and their laminates. d2344/d2344m-22. 2022.

[14] Cessna by Textron Aviation. Data sheet- cessna 172. 2010.

[15] ASTM International. Standard test method for moisture absorption properties and equilibrium conditioning of polymer matrix composite materials. d5229/d5229m-20. 2020.

[16] Weather Spark. Climate and average weather year round in singapore, 2022.

[17] Meteorological Service Singapore GOV. Climate of singapore, 2015.

[18] ASTM International. Standard practice for freeze/thaw conditioning of pultruded fiber reinforced polymer (frp) composites used in structural designs.d7792/d7792m-15. 2015.

[19] S.C. Garcea, Y. Wang, and P.J. Withers. X-ray computed tomography of polymer composites. *Composites Science and Technology*, 156:305–319, 3 2018.

[20] Giuseppe Sala. A stereo radiographic ndi technique for detection of through-the-thickness defects in composite laminates. *III ICAC International Conference. Contributo in Atti di convegno*, 10 1991.

[21] L. A. Carlsson, D. F. Adams, and R. B. Pipes. Basic experimental characterization of polymer matrix composite materials. *Polymer Reviews*, 53:277–302, 5 2013.

[22] MTS Systems. Mts 810 material test system machine data-sheet.

[23] Trevor William Clyne and Derek Hull. *An introduction to composite materials*. Cambridge university press, 2019.